Biochimica et Biophysica Acta 1858 (2016) 1868–1875

Contents lists available at ScienceDirect

Biochimica et Biophysica Acta

journal homepage: www.elsevier.com/locate/bbamem

Identification of transmembrane helix 1 (TM1) surfaces important for EnvZ dimerisation and signal output

Annika Heininger [a,1], Rahmi Yusuf [b,1], Robert J. Lawrence [b], Roger R. Draheim [b,c,*]

[a] Institute of Biochemistry, Biocenter, Goethe University Frankfurt, D-60438 Frankfurt, Germany
[b] School of Pharmacy and Biomedical Sciences, University of Portsmouth, Portsmouth PO1 2DT, England, UK
[c] Institute of Biomedical and Biomolecular Science, University of Portsmouth, Portsmouth PO1 2DT, England, UK

ARTICLE INFO

Article history:
Received 2 December 2015
Received in revised form 12 April 2016
Accepted 3 May 2016
Available online 4 May 2016

Keywords:
EnvZ signalling
Porin regulation
Osmosensing
Sulfhydryl-reactivity
Transmembrane communication

ABSTRACT

The *Escherichia coli* sensor kinase EnvZ modulates porin expression in response to various stimuli, including extracellular osmolarity, the presence of procaine and interaction with an accessory protein, MzrA. Two major outer membrane porins, OmpF and OmpC, act as passive diffusion-limited pores that allow compounds, including certain classes of antibiotics such as β-lactams and fluoroquinolones, to enter the bacterial cell. Even though the mechanisms by which EnvZ detects and processes the presence of various stimuli are a fundamental component of microbial physiology, they are not yet fully understood. Here, we assess the role of TM1 during signal transduction in response to the presence of extracellular osmolarity. Various mechanisms of transmembrane communication have been proposed including rotation of individual helices within the transmembrane domain, dynamic movement of the membrane-distal portion of the cytoplasmic domain and regulated intra-protein unfolding. To assess these possibilities, we have created a library of single-Cys-containing EnvZ proteins in order to facilitate sulfhydryl-reactivity experimentation. Our results demonstrate that the major TM1–TM1′ interface falls along a single surface consisting of residue positions 19, 23, 26, 30 and 34. In addition, we show that Cys substitutions within the N- and C-terminal regions of TM1 result in drastic changes to EnvZ signal output. Finally, we demonstrate that core residues within TM1 are responsible for both TM1 dimerisation and maintenance of steady-state signal output. Overall, our results suggest that no major rearrangement of the TM1–TM1′ interface occurs during transmembrane communication in response to extracellular osmolarity. We conclude by discussing these results within the frameworks of several proposed models for transmembrane communication.

1. Introduction

Multidrug resistance (MDR) is a frequent problem associated with nosocomial infections that limits therapeutic options [1]. In Europe, antibiotic-resistant infections kill nearly 25,000 patients and represent a total expenditure of approximately 1.5 billion € per year [2]. Surprisingly, given the seriousness of these issues, our understanding of several key molecular mechanisms involved in conferring MDR to Gram-negative bacteria remains inadequate. The outer membrane (OM) is the first line of defence for Gram-negative bacteria and serves as a major barrier that restricts access of antibiotics to the cytoplasm. The OM is impermeable to large, charged molecules and influx is largely controlled by porins, which are water-filled open channels that span the outer membrane [3–5]. β-Lactams and fluoroquinolones are prominent groups in our current antibacterial arsenal and porins serve as their major pathway for entry into the cell [6]. Thus, it should not be surprising that expression of these porins is often altered in clinical isolates that exhibit MDR [7–13]. This is highlighted by a study of *Klebsiella pneumoniae* isolates collected from different patients undergoing antibiotic treatment. In all isolates, modified outer membrane permeability was observed. In most cases, OmpK35, which belongs to the OmpF porin family that has a larger channel size, was replaced with OmpK36, which belongs to the OmpC family and possesses a smaller channel size [4].

EnvZ of *Escherichia coli* is a canonical sensor histidine kinase (SHK) that responds to changes in the extracellular osmolarity of inner-membrane impermeable compounds such as sucrose, or the presence of certain lipophilic compounds, *e.g.* procaine, by modulating the intracellular level of phosphorylated OmpR, its cognate response regulator (RR) (Fig. 1A) [14–17]. Subsequently, phospho-OmpR regulates the transcription of a number of genes, including those encoding two

Abbreviations: TM1, first transmembrane helix; MDR, multidrug resistance; OM, outer membrane; SHK, sensor histidine kinase; TM2, second transmembrane helix; HAMP, domain found in histidine kinases, adenylate cyclases, MAP kinases and phosphatases; CFP, cyan fluorescent protein; YFP, yellow fluorescent protein; IPTG, isopropyl-β-thio-galactopyranoside; NEM, *N*-ethylmaleimide; EDTA, ethylenediaminetetraacetic acid; SDS-PAGE, sodium dodecyl sulphate-polyacrylamide gel electrophoresis; ATP, adenosine triphosphate.

* Corresponding author at: University of Portsmouth, School of Pharmacy and Biomedical Sciences, St. Michael's Building, White Swan Road, Portsmouth PO1 2DT, UK.
E-mail addresses: heininger.annika@t-online.de (A. Heininger), rahmi.yusuf@port.ac.uk (R. Yusuf), robert.lawrence@port.ac.uk (R.J. Lawrence), roger.draheim@port.ac.uk (R.R. Draheim).

[1] These authors contributed equally.

http://dx.doi.org/10.1016/j.bbamem.2016.05.002
0005-2736/

major outer membrane porins, OmpF and OmpC. At low intracellular levels of phospho-OmpR (OmpR-P), transcription of *ompF* is upregulated, whereas at higher levels of OmpR-P, transcription of *ompF* is repressed and transcription of *ompC* is activated. This results in a predominance of OmpF at low osmolarity and OmpC at higher osmolarities (Fig. 1B) [18–20]. Most porins involved in antibiotic transport by Gram-negative bacteria belong to these classical OmpF and OmpC families [4]. Dramatic modification of the ratio of porin expression, also known as porin balance, which can occur during antibiotic treatment, strongly suggests that the underlying mechanisms of porin regulation by EnvZ need further characterisation.

The molecular mechanisms of perception and response to various classes of stimuli by EnvZ have long been studied but remain somewhat unclear and occasionally contradictory. Detection of and allosteric processing of intracellular osmolarity are perhaps the most well-characterised cognate stimulus of EnvZ. A recent "stretch-relaxation" model has been proposed, in which increased intracellular osmolarity promotes a more folded conformation due to increased stabilisation of intra-helical hydrogen bonding [21,22]. This conformation facilitates enhanced rates of autophosphorylation and phosphotransfer to OmpR. The authors also demonstrate that the cytoplasmic domain of EnvZ ($EnvZ_c$) alone is sufficient for osmosensing *in vivo*, leading to a proposal that the periplasmic and transmembrane (TM) domains are unnecessary for osmosensing [21,22]. However, two other research narratives suggest roles for the periplasmic or TM domain of EnvZ during detection and response to MzrA, a protein that interacts with the periplasmic domain of EnvZ, and procaine or other lipophilic compounds that potentially interacts with the transmembrane domain of EnvZ. A "gearbox"-type model proposes that a rotation of the second transmembrane helix (TM2), which physically connects the stimulus-perceiving periplasmic domain to the cytoplasmic HAMP domain and domains required for intracellular signalling, is responsible for transmembrane communication [23,24]. This model is supported by experimentation with various chimeric receptors composed of the periplasmic and TM domains from the aspartate chemoreceptor of *E. coli* (Tar) and the cytoplasmic domains of EnvZ, respectively, in which modulation of EnvZ signal output upon the addition of aspartate, the cognate ligand of Tar, has been demonstrated [25,26]. Additionally, recent studies have identified MzrA (modulator of EnvZ and OmpR protein A), a small inner membrane protein that interacts with the periplasmic domain of EnvZ *in vivo* resulting in increased EnvZ signal output [27,28]. Although porin expression in *E. coli* cells lacking (Δ*mzrA*) or overexpressing MzrA was drastically different than that in wild-type cells, modulation of porin expression due to changes in extracellular osmolarity still occurred in the absence or during overexpression of MzrA. Therefore, these results suggest that MzrA and osmosensing act independently to modulate signal EnvZ output [27,28]. Based on these different models of transmembrane communication, it remains important to better understand the role of the TM domain during stimulus processing by EnvZ in order to predict how porin balance can be targeted for direct manipulation in bacteria exhibiting MDR.

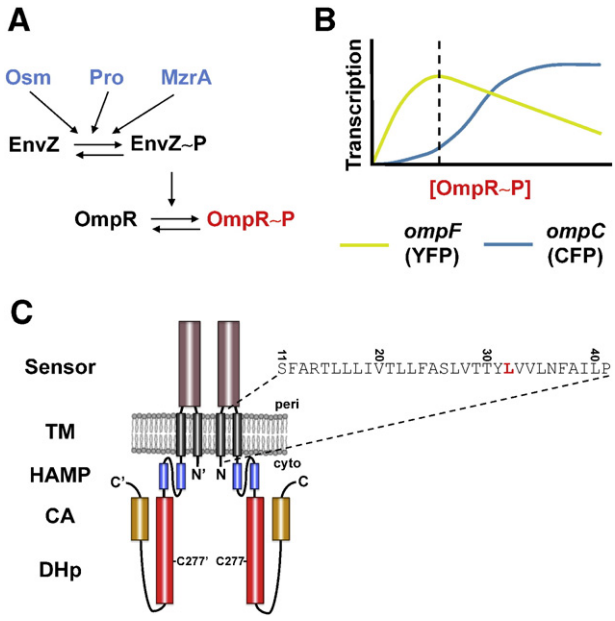

Fig. 1. The EnvZ/OmpR osmosensing circuit regulates porin expression. (A) EnvZ is bifunctional and possesses both kinase and phosphatase activity. The ratio of these activities is modulated by the presence of extracellular osmolarity [14,15], procaine [72] or MzrA [27,28]. OmpR serves as the cognate response regulator (RR) of EnvZ and thus the intracellular level of phosphorylated OmpR (OmpR-P) is governed by EnvZ activity. (B) OmpR-P levels control transcription of *ompF* and *ompC*, which can be monitored by employing MDG147 [35] or EPB30 [36] cells that contain a transcriptional fusion of *yfp* to *ompF* (yellow) and of *cfp* to *ompC* (blue). This allows the intracellular levels of OmpR-P (red) to be estimated by monitoring the CFP/YFP ratio. The dashed line represents the baseline level of OmpR-P from EPB30/pRD400 cells expressing wild-type EnvZ grown under the low-osmolarity regime (0% sucrose). (C) EnvZ functions as a homodimer with a cytoplasmic N-terminus, the first transmembrane helix (TM1, grey), a large periplasmic domain (brown), the second transmembrane helix (TM2, grey), a membrane-adjacent HAMP domain (blue) and the cytoplasmic domains responsible for dimerisation and histidylphosphotransfer (DHp, red) and catalytic ATPase activity (CA, orange). The residues subjected to Cys substitution are highlighted. Leu-32, indicated in red, could not be substituted for a Cys residue. In addition, the location of the original Cys residue at position 277 is provided.

Here, we focused on the TM domain due to its possible interaction with procaine or other lipophilic compounds. In addition, the TM domain resides between the periplasmic domain responsible for interaction with MzrA and the cytoplasmic domain responsible for intracellular signal transduction. Furthermore, several dynamic roles for TM1 and/or TM1′ have been observed. For example, a rotation between TM1 and TM1′ within McpB, a major chemoreceptor within *Bacillus subtilis*, was seen upon addition of arginine, its cognate stimulus [29]. Also, comparison of the *apo* and ligand-bound conformations of the periplasmic domains of the nitrate/nitrite sensor NarX and the TMAO-binding TorT–TorS complex suggest that TM1 plays an active role in transmembrane communication [30,31]. Finally, a scissor-type model has recently been proposed in cation −/antimicrobial peptide-binding PhoQ, which also involves dynamic movement by TM1 [32]. In order to generate a more complete understanding of the organisation of TM domain and its role during stimulus perception and processing, we created a library of EnvZ receptors that each contains a single Cys substitution between positions 11 and 41 and thus encompasses the entire region expected to comprise TM1. We demonstrated that placing a Cys residue N- and C-terminal to an internal core of 18 residues resulted in increased EnvZ signal output. Within this internal core, a surface of three adjacent residues (positions 23, 27 and 30) was identified as being intolerant of Cys substitution, in which EnvZ adopted an increased steady-state signal output. We also mapped the surface responsible for TM1 dimerisation, which was found to be composed primarily of residues 19, 23, 26, 30, and 34. Interestingly, we did not observe any significant differences in the apparent TM1–TM1′ interface when cells were grown under either the low- or high-osmolarity regime. We conclude by examining these results within the context of various models of transmembrane communication by sensor histidine kinases.

2. Materials and methods

2.1. Bacterial strains and plasmids

E. coli strain MC1061 [F- *hsdR2*(r_{K-} m_{K+}) *mcrA0 mcrB1*] [33] was used for all DNA manipulations, while strain MG1655 (F^- λ^- *ilvG rfb50 rph1*) [34] was used to control for light scattering and cellular autofluorescence. *E. coli* strains MDG147 [MG1655 Φ(*ompF*$^+$-*yfp*$^+$) Φ(*ompC*$^+$-*cfp*$^+$)] [35] and EPB30 (MDG147 *envZ*::*kan*) [36] were used for analysis of steady-state signal output from osmosensing circuits. Plasmid pRD400 [37]

retains the IPTG-based induction of EnvZ originally present in plasmid pEnvZ [38] while also encoding a seven-residue linker (GGSSAAG) [39] and a C-terminal V5 epitope tag (GKPIPNPLLGLDST) [40]. Plasmid pEB5 [41] served as an empty control vector that does not express EnvZ.

2.2. Selection of residues comprising TM1 of EnvZ

The primary sequence of EnvZ (NP_417863.1) from *E. coli* K-12 MG1655 was subjected to a full protein scan with DGpred using a minimal window of 9 residues and a maximal window of 40 residues [42]. This software searched for putative TM helices by employing a sliding window of variable lengths and calculating the ΔG_{app} for transmembrane insertion throughout the length of the sequence and suggested that residues between Phe-12 and Val-34 comprise TM1. Alternatively, a software package that identifies TM helices with a Markov model (TMHMM v2.0) [43] was employed and suggested that the residues between Thr-15 and Phe-37 compose TM1. In both cases, a motif commonly found within TM helices that consisted of positively charged residues and adjacent aromatic resides bracketing a core of aliphatic residues was found within the putative TM segments [44]. Based on these observations and to maximise the probability of including all residues within TM1, we elected to target all residues between positions 11 to 41 for the creation of a library of single-Cys-containing EnvZ receptors.

2.3. Analysis of EnvZ signal output in vivo

Bacterial cultures were grown as described previously [37] with slight modifications. Briefly, MDG147 or EPB30 cells were transformed with pRD400 expressing EnvZ that contains a Cys residue at the desired position or pEB5, as required. Fresh colonies were used to inoculate 2-ml overnight culture of minimal medium A [45] supplemented with 0.2% glucose. Ampicillin, sucrose and IPTG were added where appropriate. Cells were grown overnight at 37 °C and diluted at least 1:1000 into 7-ml of fresh medium. When the final bacterial cultures reached an OD_{600nm} ~0.3, chloramphenicol was added to a final concentration of 170 μg/ml to inhibit protein synthesis. Fluorescent analysis was immediately conducted with 2 ml of culture. All fluorescence measurements were performed with a Varian Cary Eclipse (Palo Alto, CA). CFP fluorescence was measured using an excitation wavelength of 434 nm and an emission wavelength of 477 nm, while YFP fluorescence was measured using an excitation wavelength of 505 nm and an emission wavelength of 527 nm. These values were corrected for differences in cell density by dividing the fluorescent intensities by OD_{600nm} and for light scattering/cellular autofluorescence by subtracting the CFP and YFP fluorescence intensities determined for MG1655/pEB5 cells.

2.4. Analysis of sulfhydryl-reactivity in vivo

Cells were grown as described above with minor modifications. Upon reaching an OD_{600nm} ~0.3, cells were subjected to between 10 and 250 μM molecular iodine (as required) for between 1 and 10 min (as required) while incubating at 37 °C. The reaction was terminated with 8 mM *N*-ethylmaleimide (NEM) and 10 mM EDTA. Cells were harvested by centrifugation and resuspended in standard 6X non-reducing SDS-PAGE buffer supplemented with 12.5 mM NEM. Cell pellets were then analysed on 10% SDS/acrylamide gels. Standard buffers and conditions were used for electrophoresis, immunoblotting and detection with enhanced chemiluminescence [46]. Anti-V5 (Invitrogen) was used as the primary antibody, while peroxidase-conjugated anti-mouse IgG (Sigma) was employed as the secondary antibody. Digitised images were acquired with a ChemiDoc MP workstation (Bio-Rad), analysed with ImageJ v1.49 [47] and quantified with QtiPlot v0.9.8.10.

3. Results

3.1. Overview of sulfhydryl-reactivity analysis

One of our primary interests is to determine how the transmembrane (TM) domain of EnvZ allosterically processes and couples different sensory inputs into a single unified output. To determine which residues of EnvZ compose TM1, we subjected the primary sequence to a full protein scan with DGpred [42], which suggested that residues Phe-12 to Val-34 comprise TM1. We also employed TMHMM v2.0 [43], which suggested that the residues between Thr-15 and Phe-37 compose TM1. These results are similar to previously proposed TM1 composition [48,49], therefore, we employed sulfhydryl-reactivity experimentation between residue positions 11 and 41 in order to ensure that the entire first transmembrane helix (TM1) was encompassed.

Sulfhydryl-reactivity possesses several distinct advantages. Firstly, it is well-characterised and has been employed on many soluble and membrane-spanning proteins and higher-order complexes [50]. Based on these previous results, we have been able to compare our results with those from other membrane-spanning receptors. Secondly, these reactions can be performed *in vivo*, which allows EnvZ to remain within its native environment while retaining the ability to adjust extracellular osmolarity. In addition, this leaves all accessory proteins, such as MzrA, present and modulatable within the host cell membrane. Finally, the use of an *in vivo* methodology allowed us to monitor signal output with a dual-colour fluorescence-based system that we, and other groups, have previously employed to determine which surfaces of TM1 are intolerant of Cys substitutions [35,37,41]. In summary, the *in vivo* nature of this assay facilitated mapping of the TM1–TM1′ interface under different osmotic conditions, which is an important first step toward understanding how EnvZ processes different allosteric signal inputs into a single uniform modulation of bacterial porin balance.

3.2. Creation of a cysteine-less EnvZ (Cys-less)

Wild-type EnvZ from *E. coli* contains a single cysteine residue at position 277 (Fig. 1C). Pre-existing Cys residues would make it significantly more difficult to interpret the results of *in vivo* disulphide-mapping experimentation, therefore, we created a cysteine-less (Cys-less) version of EnvZ. The native Cys-277 codon was converted to a methionine (C277M) because a previous sequence analysis determined that a Met residue was the second most common, after Cys, at position 277 within EnvZ proteins from other organisms [51]. A Ser residue was also chosen (C277S) because it was shown to not affect the biochemical activities of the purified cytoplasmic domain from *E. coli* ($EnvZ_c$) [52]. Finally, as a small non-polar residue, an Ala (C277A) was also selected for analysis. All substitutions were made using standard site-directed mutagenesis techniques and expressed from pRD400 [37], which results in the addition of a seven-residue linker (GGSSAAG) and a C-terminal V5 epitope (GKPIPNPLLGLDST) that have previously been used within bacterial receptors, including Tar and EnvZ, resulting in minimal effect to steady-state signal output [37,39,53–58].

To measure steady-state signal output from EnvZ/OmpR osmosensing circuits possessing the Cys-less variants, two-colour fluorescent reporter strains were used. MDG147 is a derivative of *E. coli* strain K-12 MG1655 that possesses transcriptional fusions of *cfp* to *ompC* and of *yfp* to *ompF* within its chromosome. This allows the ratio of CFP to YFP fluorescence (CFP/YFP) to provide a rapid and sensitive measure of the ratio of *ompC* to *ompF* transcription, which estimates the intracellular level of phosphorylated OmpR (Fig. 1B) [35,37,41]. MDG147 cells harbouring the empty vector pEB5 [41] were grown in glucose minimal medium under either the low- (0% sucrose) or high- (15% sucrose) osmolarity regime and both CFP fluorescence and YFP fluorescence were measured. As previously observed, an increase in CFP fluorescence along with a concomitant decrease in YFP fluorescence, resulting in an increased CFP/

YFP ratio, was observed when MDG147/pEB5 cells were grown under the high-osmolarity regime (Fig. 2A and B) [35,37].

To assess whether plasmid-based complementation could produce similar steady-state signal output, EPB30 (MDG147 *envZ*::*kan*) cells [36] were complemented with the Cys-less EnvZ variants expressed from plasmid pRD400 [37]. EPB30/pRD400 cells expressing the C277M variant resulted in CFP and YFP fluorescence similar to those harbouring the control vector (EPB30/pEB5) under both osmotic regimes, therefore, it was not considered for further analysis (Fig. S1). The C277A variant facilitated steady-state output similar to plasmid-based wild-type EnvZ under both regimes, while C277S resulted in slightly lower steady-state signal output (Fig. S2). Based on these results, we elected to continue with the C277A under conditions that produced results similar to MDG147/pEB5 cells (Figs. 2A, B and S2).

3.3. Mapping TM1 surfaces responsible for maintenance of EnvZ signal output

As described above, positions 11 through 41 were selected to ensure that all residues potentially comprising TM1 were converted to a Cys residue. A library of single-Cys-containing EnvZ proteins was created by employing standard site-directed mutagenesis using pRD400 containing the C277A variant as a template (Fig. 2). Although several attempts were made, a Cys residue could not be placed at position 32. We observed that the entire library, with a few exceptions, was expressed within EPB30/pRD400 cells grown under the low- or high-osmolarity regime (Fig. S4). Under both the low- and high-osmolarity regimes the L23C variant was found at significantly lower steady-state levels. In addition, the monomeric form of the P41C variant was only quantifiable when EPB30/pRD400 cells were grown under the high-osmolarity regime (Fig. S4).

For EPB30/pRD400 cells each expressing a single-Cys-containing receptor, we measured CFP fluorescence, YFP fluorescence and also calculated the CFP/YFP ratio, which serves as an estimate of steady-state EnvZ signal output. EPB30/pRD400 cells expressing the C277A variant were used as the baseline for comparison (Figs. 2A, B and S2). Under the low-osmolarity regime, a shift in signalling output toward the "on" state results in increased CFP fluorescence (Fig. S3A), decreased YFP fluorescence (Fig. S3B) and an overall increase in the CFP/YFP ratio (Fig. 3A and B), while a shift toward the "off" state appears as decreased CFP (Fig. S3A), increased YFP (Fig. S3B) and a decrease in CFP/YFP ratio (Fig. 3A and B).

Several trends were observed during analysis of the entire single-Cys-containing library. When EPB30/pRD400 cells were grown under the low-osmolarity regime, EnvZ was less tolerant of Cys substitutions at the N- and C-terminal regions of the library. In most cases, this results

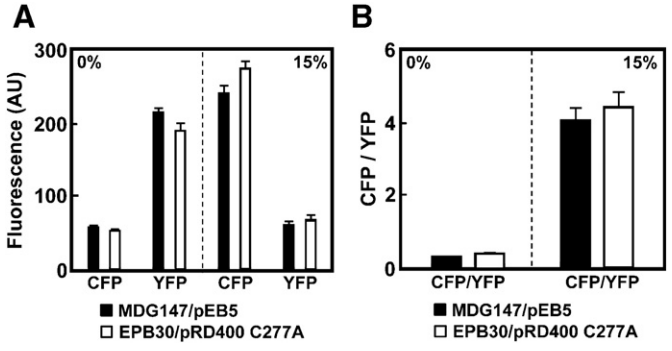

Fig. 2. Signal output of the Cys-less variant of EnvZ. (A) CFP and YFP fluorescence from MDG147/pEB5 (filled) and EPB30/pRD400 C277A (Cys-less; empty) cells grown under the low- (0% sucrose) and high-osmolarity (15% sucrose) regimes. (B) The CFP/YFP ratio from MDG147/pEB5 (filled) and EPB30/pRD400 C277A (Cys-less; empty) cells grown under the low- and high-osmolarity regimes estimates EnvZ signal output. Error bars represent standard deviation of the mean with a sample size of n ≥ 3.

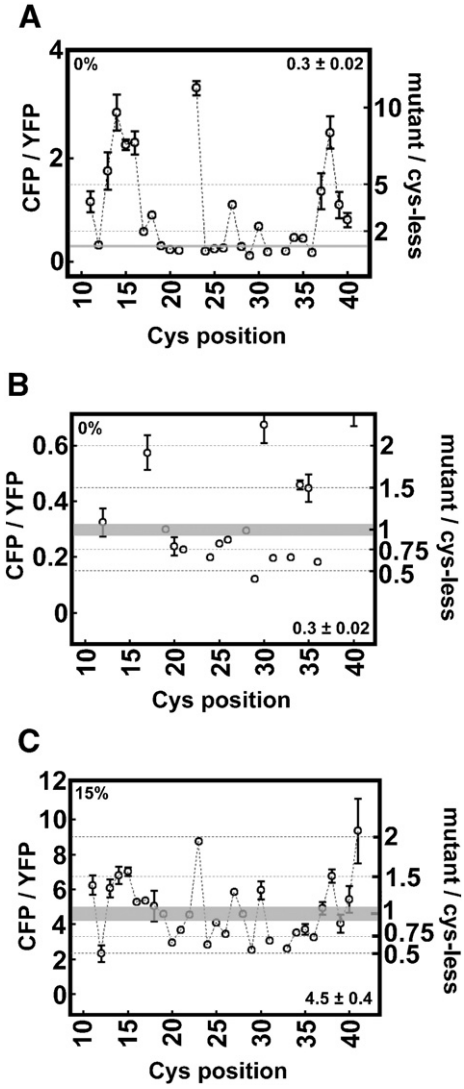

Fig. 3. Signal output from the library of single-Cys-containing EnvZ variants. (A) CFP/YFP ratios from EPB30/pRD400 cells expressing one of the single-Cys-containing EnvZ variants grown under the low-osmolarity (0% sucrose) regime. These ratios are also compared to EPB30/pRD400 cells expressing the Cys-less (C277A) variant and are used to demarcate the Cys-containing variants in Fig. 5B. (B) Magnified version of panel A in order to emphasise the region up to a 2-fold increase in CFP/YFP over cells expressing the Cys-less variant. (C) CFP/YFP ratios from EPB30/pRD400 cells expressing one of the single-Cys-containing EnvZ variants grown under the high-osmolarity (15% sucrose) regime. These ratios are also compared to EPB30/pRD400 cells expressing the Cys-less (C277A) variant and are used to demarcate the Cys-containing variants in Fig. 5B. It is important to note that cells expressing the P41C variant were analysed only when grown under the high-osmolarity regime. The shaded areas represent the mean and a range of one standard deviation of mean. These values are provided to aid in comparison. Error bars represent standard deviation of the mean with a sample size of n ≥ 3.

in a shift toward the "on" state of EnvZ, demonstrated by an increase in CFP fluorescence and a decrease in YFP fluorescence. These boundary regions appear to flank a core of alternating increases and decreases in EnvZ signal output, suggesting that multiple tightly packed EnvZ helices exist within the hydrophobic core of the inner membrane. It should also be noted that when EPB30/pRD400 cells were grown under the low-osmolarity regime, a Cys at residue position 22 prevented cellular growth, however, this was not observed when cells were grown under the high-osmolarity regime (Figs. 3, S3 and S4). Interestingly, these results occurred adjacent to the position that possessed the most-biased steady-state signal output (Cys-23). When EPB30/pRD400 cells were grown under the high-osmolarity regime, we observed a similar pattern of changes in the CFP fluorescence (Fig. S3C), YFP

fluorescence (Fig. S3D) and in CYP/YFP ratio (Fig. 3C), however, these changes were smaller in magnitude, perhaps due to the fact that the EnvZ/OmpR circuit was already activated and thus disturbances due to altered surface interactions would be of a smaller magnitude.

3.4. Identifying surfaces involved in TM1–TM1′ dimerisation

Based on the effect of the individual Cys substitutions on EnvZ signal output, it appears that a potential helix is formed within the hydrophobic core of the membrane. Therefore, we were interested in determining whether the helical surface participating in TM1–TM1′ interaction surface could be identified. To accomplish this, the library of single-Cys-containing variants was expressed in EPB30/pRD400 cells and upon reaching an OD_{600nm} of approximately 0.3, cells were subjected to 250 μM molecular iodine for 10 min and subsequently analysed by non-reducing SDS-PAGE. These conditions have been previously shown to promote disulphide formation in various membrane-spanning receptors *in vivo* [50]. Upon comparison of the wild-type and the C277A variant, under either osmotic regime, the presence of a higher molecular weight band confirmed the necessity of Cys-277 removal (Fig. S5).

Based on these results, EPB30/pRD400 cells expressing the single-Cys-containing EnvZ variants were grown under the low- (0% sucrose) and high-osmolarity (15% sucrose) regimes and subjected to molecular iodine, non-reducing SDS-PAGE and immunoblotting against the C-terminal V5 epitope (Fig. S6). Data were tabulated for every position with the exception of residue position 32, which could not be made as described above. We observed three regions, each with a different extent of disulphide bond formation. The N-terminal region (region I in Fig. 4), comprising residues 11 to 18, exhibited almost no crosslinking, except for a minimal amount at positions 11 and 15. The second region (II), consisting of positions 19 to 37, demonstrated alternating low and high levels of disulphide formation consistent with the hydrophobic core of TM1. The final region (III) consists of the C-terminal periplasmic positions in our library, residues 38 through 41, where the apparent helical pattern is interrupted and an overall greater extent of sulfhydryl-reactivity is observed. Altering the reaction conditions as shown in Figs. S7 and S8 further supported the differentiation of the TM1 into Regions I through III.

4. Discussion

4.1. Establishing the surface of TM1 that promotes dimerisation

The results of sulfhydryl-reactivity experiments were plotted on a helical net [59] to visualise the TM1–TM1′ interaction surface. Using the well-defined distance and angular constraints of a disulphide bond [60,61], we assessed the relative distance between Cys residues along the TM1–TM1′ interface. These constraints can be estimated from the distance between β-carbons in disulphide bonds, which range from 3.4 to 4.6 Å in protein crystal structures [62]. Therefore, when we employ a fixed concentration of molecular iodine (250 μM) and reaction time (10 min), the extent of crosslinking correlates with the distance between the Cys residues (Fig. S6). Based on this correlation, residue positions 23/23′ and 26/26′ would be in closest proximity. By extension, the significant reduction in crosslinking as the Cys residues become more distal from these positions within the membrane core suggests that the TM1 and TM1′ helices cross at an angle that results in increased distance between residues near the membrane boundaries. Therefore, we propose that the major TM1–TM1′ interaction surface consists of residues Ile-19, Leu-23, Ser-26, Thr-30 and Val-34 (Fig. 5A). In addition, minor reactivity was observed with residues Ser-11 and Thr-15, suggesting that they are quite distant but most likely reside on the same surface as the TM1–TM1′ interface. Adjacent residues at the periplasmic end of TM1, ranging from position 38 to 40 also exhibited extensive cross-linking, however the helical pattern was interrupted suggesting that a less uniform structure exists within these residues (Figs. 4 and 5A). Also important to note is that no significant differences in the TM1–TM1′ interface were observed when cells were grown under the low- (0% sucrose) or high-osmolarity (15% sucrose) regime (Fig. 4).

We believe that the residues examined can be formally divided into three distinct regions (Fig. 5A) based on the results obtained when changing the concentration of iodine (Fig. S7) or the reaction time (Fig. S8). The EnvZ variants within Region I (S11C and T15C) follow a distinct pattern of forming disulphide bonds only in the presence of the highest concentration of iodine (250 μM) and the longest duration (10 min). These data suggest that the Cys residues are either very distant, such that they irregularly form a disulphide bond, or are internal to the inner leaflet of the cytoplasmic membrane. The variants in Region II (I19C, L23C, S26C, T30C, V34C and A25C to a minor extent) all follow a similar pattern that is different than the variants in the first region. Here, a minor extent of crosslinking at the distal ends of the region, namely I19C and V34C, is observed, while a maximal amount is seen near the core that is comprised of L23C and S26C. This is further demonstrated by comparing the extent of crosslinking at the higher concentrations of iodine (100 μM and 250 μM). In addition, unlike residues in Region I, the reaction is complete after 1 min regardless of the overall extent of crosslinking (Fig. S8). The variants found in Region III (A38C, I39C and L40C) follow a third distinct pattern. EnvZ A38C exhibited a much greater extent of crosslinking than V34C, and thus does not conform to the crossing helix pattern. In addition, EnvZ I39C and L40C show crosslinking at all concentrations of iodine (Fig. S7) and thus suggest that either the helix becomes broken/unwound, or that these residues reside in the periplasm, or both. It is also worth noting that when cells were grown under the low osmolarity regime and in the absence of iodine (Fig. S4), crosslinking occurred at positions 38 through 40, suggesting that they may reside within the oxidising environment of the periplasm.

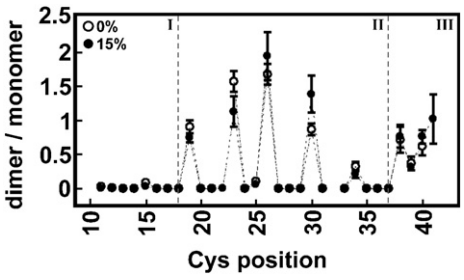

Fig. 4. Extent of sulfhydryl-reactivity for each single-Cys-containing variant. EPB30/pRD400 cells growing under the low- (empty circles, 0% sucrose) or high-osmolarity (filled circles, 15% sucrose) regimes were analysed to determine the ratio of dimeric:monomeric EnvZ at each position as shown in Fig. S6. As described within the text, three distinct regions (I, II and III) were observed. Error bars represent standard deviation of the mean with a sample size of n ≥ 3.

4.2. Mapping surfaces of TM1 responsible for maintenance of baseline EnvZ signal output

In order to visualise which surfaces of TM1 are responsible for maintenance of steady-state EnvZ signal output, we mapped the signal output of the family of single-Cys-containing receptors onto a helical net (Fig. 5B). This analysis resulted in the identification of three subdomains intolerant of Cys substitutions (signal output greater than 150% of the Cys-less variant): the cytoplasmic end of TM1 (Surface I), three residues in the core of the membrane (Surface II) and the periplasmic end of TM1 (Surface III). We did not consider surfaces II and III as contiguous because surface III may be due to breaching the periplasmic boundary, while surface II remained buried but truly intolerant of Cys substitution. This becomes more clear when cells are grown under the high-osmolarity (15% sucrose) regime (Fig. 5B). It is also important to emphasise that the two residues in the membrane core (positions 17

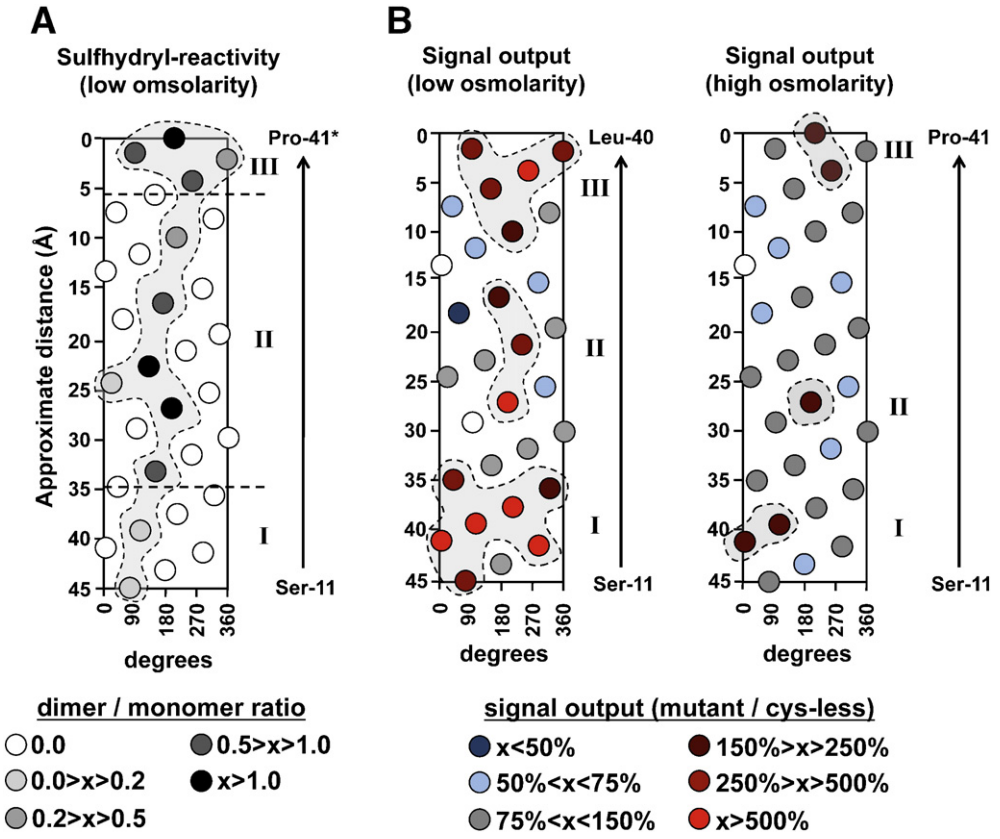

Fig. 5. Helical net diagrams illustrating the TM1–TM1′ interface and surfaces important for maintenance of baseline EnvZ signal output. (A) The TM1–TM1′ interface remains similar when EPB30/pRD400 cells are grown under the low- (0% sucrose) or high-osmolarity (15% sucrose) regime. The extent of TM1-TM1' crosslinking, measured as the ratio of dimeric:monomeric EnvZ moieties at each position is represented by the intensity of darkness. Residue positions 23 and 26, which reside in close proximity, result in the greatest extent of cross-linking. As the position of the Cys residue is moved toward the cytoplasmic end of the helix, a decrease in reactivity is observed. The divergence from a helical pattern at the periplasmic end of TM1 may indicate that the periplasmic boundary of the membrane has been breached and/or that the helicity is not observed within this region. It should be noted that the P41C, indicated with an asterisk, variant could only be analysed when grown under the high-osmolarity regime. (B) Cys substitutions that result in decreased signal output compared to the cys-less variant are presented in blue colours, while those resulting in increased signal output are indicated in red. Regions responsible for maintenance of baseline signal output fall into three contiguous surfaces (red dots residing under a transparent grey area): one at the cytoplasmic end (surface I), a small one within the membrane core (surface II) and one at the periplasmic end of the helix (surface III). These surfaces are less pronounced when cells are grown under the high-osmolarity regime, possibly because the EnvZ/OmpR circuit is already stimulated by external osmolarity. The white circles represent the Cys-32 mutant that could not be created and the Cys-22 variant that failed to grow under the low-osmolarity regime.

and 24) are subject to both sulfhydryl-reactivity and intolerance of Cys substitution with regard to steady-state signal output. Overall, similar patterns were observed when EPB30/pRD400 cells were grown under the high-osmolarity regime (15% sucrose), although the degree of increased signal output was smaller, perhaps because the EnvZ/OmpR circuit was already activated (Fig. 5B).

Two EnvZ mutants that reside within the region we analysed (V33E and P41L) were previously shown to result significantly greater increased steady-state signal output [63,64]. Our data with EnvZ P41C is in agreement with the previously published results with P41L, which demonstrates that the loss of the Pro residue results in greatly increased steady-state EnvZ signal output. In fact, the P41C variant of EnvZ results in the greatest change in signal output when grown under the high-osmolarity regime (Fig. 3). However, with EnvZ V33C, we observed different results than those previously published with the V33E variant. This difference suggests that the loss of Val-33 is not the major driving force for changing steady-state signal output and that the increased activation is most likely due to the insertion of a Glu residue. This is not unexpected as we previously demonstrated [65] that residues with longer side chains within their R-group possess the ability to snorkel and interact with, or be repulsed from in this case, the negatively charged phospholipid head groups in the cytoplasmic membrane. This may explain why our V33C variant did not exhibit similar properties to the previously published EnvZ V33E.

4.3. Evaluation within the context of current models for transmembrane communication

These data demonstrate that the TM1–TM1′ interface does not significantly change when EPB30/pRD400 cells are grown under regimes possessing different osmolarities (Fig. 4). This suggests that TM1–TM1′ might be relatively static in a manner consistent with results previously observed with the aspartate and ribose/galactose chemoreceptors [66] and also recently with DcuS, the C_4-dicarboxylate sensor of *E. coli* [67]. However, other types of signalling mechanisms that involve more dynamic roles for TM1 and/or TM1′ have been observed. For example, a rotation between TM1 and TM1′ within McpB of *B. subtilis* was seen upon addition of arginine [29], its cognate stimulus, whereas our results suggest that no rotation occurs along the TM1–TM1′ interface in response to osmolarity. In addition, small piston-type displacements of TM1 have been observed in the periplasmic domain of NarX and the TorT-TorS complex [30,31] and these might not be detectable within the current iteration of our assay.

From another perspective, our results are in agreement with recent analyses involving PhoQ that proposed the existence of water-filled hemichannel spanning through the cytoplasmic end of the TM domain [68]. Our data suggesting that TM1 and TM1' cross at an angle resulting in an increasing distance between the residues as they become further distal from the membrane core is consistent with the presence of

water hemichannel possessing a cytoplasmic-facing opening. The proposed necessity of a polar residue is also consistent with our previous results involving "aromatic tuning" and the repositioning of non-polar hydrophobic residues around the cytoplasmic end of TM2 resulting in modified signal output [37,65,69]. Recently, further experimentation proposed a scissor-type model, which would also be consistent with our helical crossing angles. We are planning to undertake further experimentation to thoroughly assess these models [32]. In light of the plethora of proposed signalling mechanisms, recent publications [70,71] suggest that different subclasses of bacterial receptors may employ alternate mechanisms of signal transmission and that every proposed mechanism should not be imposed upon all bacterial membrane-spanning receptors.

Transparency document

The Transparency document related to this article can be found, in the online version.

Acknowledgements

Morag Mansley (Durham University) provided valuable insight into optimisation of the chemiluminescent reagent. Nesrine Benslimane (Université de Rouen), Tuyết Linh Nguyễn (Uniwersytet Jagielloński) and Bérénice Tendrel (Institute of Technology of Laval, University of Maine-Le Mans, France) gave the manuscript a final thorough critique. R. Y. was generously supported by the Indonesia Endowment Fund for Education, Ministry of Finance (S-4833/LPDP.3/2015). R. R. D. was supported with start-up funding from the Faculty of Science and from the Institute of Biomedical and Biomolecular Science (IBBS) at the University of Portsmouth.

Appendix A. Supplementary data

Supplementary data to this article can be found online at http://dx.doi.org/10.1016/j.bbamem.2016.05.002.

References

[1] S. Blot, P. Depuydt, K. Vandewoude, D. De Bacquer, Measuring the impact of multidrug resistance in nosocomial infection, Curr. Opin. Infect. Dis. 20 (2007) 391–396.
[2] T. Kirby, Europe to boost development of new antimicrobial drugs, Lancet 379 (2012) 2229–2230.
[3] A.H. Delcour, Solute uptake through general porins, Front. Biosci. 8 (2003) d1055–d1071.
[4] H. Nikaido, Molecular basis of bacterial outer membrane permeability revisited, Microbiol. Mol. Biol. Rev. 67 (2003) 593–656.
[5] G.E. Schulz, The structure of bacterial outer membrane proteins, Biochim. Biophys. Acta 1565 (2002) 308–317.
[6] A. Bryskier, Antimicrobial Agents: Antibacterials and Antifungals, ASM Press, Washington, DC, USA, 2005.
[7] E. Elliott, A.J. Brink, J. van Greune, Z. Els, N. Woodford, J. Turton, M. Warner, D.M. Livermore, In vivo development of ertapenem resistance in a patient with pneumonia caused by *Klebsiella pneumoniae* with an extended-spectrum beta-lactamase, Clin. Infect. Dis. 42 (2006) e95–e98.
[8] S. Hernandez-Alles, M. Conejo, A. Pascual, J.M. Tomas, V.J. Benedi, L. Martinez-Martinez, Relationship between outer membrane alterations and susceptibility to antimicrobial agents in isogenic strains of *Klebsiella pneumoniae*, J. Antimicrob. Chemother. 46 (2000) 273–277.
[9] G.A. Jacoby, D.M. Mills, N. Chow, Role of beta-lactamases and porins in resistance to ertapenem and other beta-lactams in *Klebsiella pneumoniae*, Antimicrob. Agents Chemother. 48 (2004) 3203–3206.
[10] F.M. Kaczmarek, F. Dib-Hajj, W. Shang, T.D. Gootz, High-level carbapenem resistance in a *Klebsiella pneumoniae* clinical isolate is due to the combination of bla(ACT-1) beta-lactamase production, porin OmpK35/36 insertional inactivation, and down-regulation of the phosphate transport porin phoe, Antimicrob. Agents Chemother. 50 (2006) 3396–3406.
[11] A. Loli, L.S. Tzouvelekis, E. Tzelepi, A. Carattoli, A.C. Vatopoulos, P.T. Tassios, V. Miriagou, Sources of diversity of carbapenem resistance levels in *Klebsiella pneumoniae* carrying blaVIM-1, J. Antimicrob. Chemother. 58 (2006) 669–672.
[12] L. Martinez-Martinez, M.C. Conejo, A. Pascual, S. Hernandez-Alles, S. Ballesta, E. Ramirez De Arellano-Ramos, V.J. Benedi, E.J. Perea, Activities of imipenem and cephalosporins against clonally related strains of *Escherichia coli* hyperproducing chromosomal beta-lactamase and showing altered porin profiles, Antimicrob. Agents Chemother. 44 (2000) 2534–2536.
[13] A. Mena, V. Plasencia, L. Garcia, O. Hidalgo, J.I. Ayestaran, S. Alberti, N. Borrell, J.L. Perez, A. Oliver, Characterization of a large outbreak by CTX-M-1-producing *Klebsiella pneumoniae* and mechanisms leading to in vivo carbapenem resistance development, J. Clin. Microbiol. 44 (2006) 2831–2837.
[14] L.A. Egger, M. Inouye, Purification and characterization of the periplasmic domain of EnvZ osmosensor in *Escherichia coli*, Biochem. Biophys. Res. Commun. 231 (1997) 68–72.
[15] S.A. Forst, D.L. Roberts, Signal transduction by the EnvZ-OmpR phosphotransfer system in bacteria, Res. Microbiol. 145 (1994) 363–373.
[16] T. Mizuno, His–Asp phosphotransfer signal transduction, J. Biochem. 123 (1998) 555–563.
[17] J.A. Hoch, T.J. Silhavy, Two-Component Signal Transduction, American Society of Microbiology Press, Washington, DC, USA, 1995.
[18] S.A. Forst, J. Delgado, M. Inouye, DNA-binding properties of the transcription activator (OmpR) for the upstream sequences of ompF in *Escherichia coli* are altered by envZ mutations and medium osmolarity, J. Bacteriol. 171 (1989) 2949–2955.
[19] C.Y. Lan, M.M. Igo, Differential expression of the OmpF and OmpC porin proteins in *Escherichia coli* K-12 depends upon the level of active OmpR, J. Bacteriol. 180 (1998) 171–174.
[20] F.D. Russo, T.J. Silhavy, EnvZ controls the concentration of phosphorylated OmpR to mediate osmoregulation of the porin genes, J. Mol. Biol. 222 (1991) 567–580.
[21] L.C. Wang, L.K. Morgan, P. Godakumbura, L.J. Kenney, G.S. Anand, The inner membrane histidine kinase EnvZ senses osmolality via helix-coil transitions in the cytoplasm, EMBO J. 31 (2012) 2648–2659.
[22] Y.H. Foo, Y. Gao, H. Zhang, L.J. Kenney, Cytoplasmic sensing by the inner membrane histidine kinase EnvZ, Prog. Biophys. Mol. Biol. (2015).
[23] M. Hulko, F. Berndt, M. Gruber, J.U. Linder, V. Truffault, A. Schultz, J. Martin, J.E. Schultz, A.N. Lupas, M. Coles, The HAMP domain structure implies helix rotation in transmembrane signaling, Cell 126 (2006) 929–940.
[24] M. Inouye, Signaling by transmembrane proteins shifts gears, Cell 126 (2006) 829–831.
[25] Y. Zhu, M. Inouye, Analysis of the role of the EnvZ linker region in signal transduction using a chimeric Tar/EnvZ receptor protein, Tez1, J. Biol. Chem. 278 (2003) 22812–22819.
[26] R. Utsumi, R.E. Brissette, A. Rampersaud, S.A. Forst, K. Oosawa, M. Inouye, Activation of bacterial porin gene expression by a chimeric signal transducer in response to aspartate, Science 245 (1989) 1246–1249.
[27] H. Gerken, E.S. Charlson, E.M. Cicirelli, L.J. Kenney, R. Misra, MzrA: a novel modulator of the EnvZ/OmpR two-component regulon, Mol. Microbiol. 72 (2009) 1408–1422.
[28] H. Gerken, R. Misra, MzrA-EnvZ interactions in the periplasm influence the EnvZ/OmpR two-component regulon, J. Bacteriol. 192 (2010) 6271–6278.
[29] H. Szurmant, M.W. Bunn, S.H. Cho, G.W. Ordal, Ligand-induced conformational changes in the *Bacillus subtilis* chemoreceptor McpB determined by disulfide crosslinking in vivo, J. Mol. Biol. 344 (2004) 919–928.
[30] J. Cheung, W.A. Hendrickson, Structural analysis of ligand stimulation of the histidine kinase NarX, Structure 17 (2009) 190–201.
[31] J.O. Moore, W.A. Hendrickson, Structural analysis of sensor domains from the TMAO-responsive histidine kinase receptor TorS, Structure 17 (2009) 1195–1204.
[32] K.S. Molnar, M. Bonomi, R. Pellarin, G.D. Clinthorne, G. Gonzalez, S.D. Goldberg, M. Goulian, A. Sali, W.F. DeGrado, Cys-scanning disulfide crosslinking and Bayesian modeling probe the transmembrane signaling mechanism of the histidine kinase, PhoQ, Structure 22 (2014) 1239–1251.
[33] M.J. Casadaban, S.N. Cohen, Analysis of gene control signals by DNA fusion and cloning in *Escherichia coli*, J. Mol. Biol. 138 (1980) 179–207.
[34] M.S. Guyer, R.R. Reed, J.A. Steitz, K.B. Low, Identification of a sex-factor-affinity site in *E. coli* as gamma delta, Cold Spring Harb. Symp. Quant. Biol. 45 (Pt 1) (1981) 135–140.
[35] E. Batchelor, T.J. Silhavy, M. Goulian, Continuous control in bacterial regulatory circuits, J. Bacteriol. 186 (2004) 7618–7625.
[36] A. Siryaporn, M. Goulian, Cross-talk suppression between the CpxA-CpxR and EnvZ-OmpR two-component systems in *E. coli*, Mol. Microbiol. 70 (2008) 494–506.
[37] M.H. Norholm, G. von Heijne, R.R. Draheim, Forcing the issue: aromatic tuning facilitates stimulus-independent modulation of a two-component signaling circuit, ACS Synth. Biol. 4 (2015) 474–481.
[38] W. Hsing, T.J. Silhavy, Function of conserved histidine-243 in phosphatase activity of EnvZ, the sensor for porin osmoregulation in *Escherichia coli*, J. Bacteriol. 179 (1997) 3729–3735.
[39] B.J. Cantwell, R.R. Draheim, R.B. Weart, C. Nguyen, R.C. Stewart, M.D. Manson, CheZ phosphatase localizes to chemoreceptor patches via CheA-short, J. Bacteriol. 185 (2003) 2354–2361.
[40] J.A. Southern, D.F. Young, F. Heaney, W.K. Baumgartner, R.E. Randall, Identification of an epitope on the P and V proteins of simian virus 5 that distinguishes between two isolates with different biological characteristics, J. Gen. Virol. 72 (Pt 7) (1991) 1551–1557.
[41] E. Batchelor, M. Goulian, Robustness and the cycle of phosphorylation and dephosphorylation in a two-component regulatory system, Proc. Natl. Acad. Sci. U. S. A. 100 (2003) 691–696.
[42] T. Hessa, N.M. Meindl-Beinker, A. Bernsel, H. Kim, Y. Sato, M. Lerch-Bader, I. Nilsson, S.H. White, G. von Heijne, Molecular code for transmembrane-helix recognition by the Sec61 translocon, Nature 450 (2007) 1026–1030.
[43] A. Krogh, B. Larsson, G. von Heijne, E.L. Sonnhammer, Predicting transmembrane protein topology with a hidden Markov model: application to complete genomes, J. Mol. Biol. 305 (2001) 567–580.
[44] T.K. Nyholm, S. Ozdirekcan, J.A. Killian, How protein transmembrane segments sense the lipid environment, Biochemistry 46 (2007) 1457–1465.

[45] J.H. Miller, A Short Course in Bacterial Genetics: a Laboratory Manual and Handbook for *Escherichia coli* and Related Bacteria, Cold Spring Harbor Laboratory Press, Plainview, NY, 1992.
[46] F.M. Ausubel, R. Brent, R.E. Kingston, D.D. Moore, J.G. Seidman, J.A. Smith, K. Struhl, Current Protocols in Molecular Biology, Wiley, New York, NY, 1998.
[47] C.A. Schneider, W.S. Rasband, K.W. Eliceiri, NIH Image to ImageJ: 25 years of image analysis, Nat. Methods 9 (2012) 671–675.
[48] H. Yaku, T. Mizuno, The membrane-located osmosensory kinase, EnvZ, that contains a leucine zipper-like motif functions as a dimer in *Escherichia coli*, FEBS Lett. 417 (1997) 409–413.
[49] S. Forst, D. Comeau, S. Norioka, M. Inouye, Localization and membrane topology of EnvZ, a protein involved in osmoregulation of OmpF and OmpC in *Escherichia coli*, J. Biol. Chem. 262 (1987) 16433–16438.
[50] R.B. Bass, S.L. Butler, S.A. Chervitz, S.L. Gloor, J.J. Falke, Use of site-directed cysteine and disulfide chemistry to probe protein structure and dynamics: applications to soluble and transmembrane receptors of bacterial chemotaxis, Methods Enzymol. 423 (2007) 25–51.
[51] R. Oropeza, E. Calva, The cysteine 354 and 277 residues of *Salmonella enterica* serovar Typhi EnvZ are determinants of autophosphorylation and OmpR phosphorylation, FEMS Microbiol. Lett. 292 (2009) 282–290.
[52] S.J. Cai, A. Khorchid, M. Ikura, M. Inouye, Probing catalytically essential domain orientation in histidine kinase EnvZ by targeted disulfide crosslinking, J. Mol. Biol. 328 (2003) 409–418.
[53] R.R. Draheim, A.F. Bormans, R.Z. Lai, M.D. Manson, Tryptophan residues flanking the second transmembrane helix (TM2) set the signaling state of the Tar chemoreceptor, Biochemistry 44 (2005) 1268–1277.
[54] R.R. Draheim, A.F. Bormans, R.Z. Lai, M.D. Manson, Tuning a bacterial chemoreceptor with protein-membrane interactions, Biochemistry 45 (2006) 14655–14664.
[55] G.A. Wright, R.L. Crowder, R.R. Draheim, M.D. Manson, Mutational analysis of the transmembrane helix 2-HAMP domain connection in the *Escherichia coli* aspartate chemoreceptor tar, J. Bacteriol. 193 (2011) 82–90.
[56] C.A. Adase, R.R. Draheim, M.D. Manson, The residue composition of the aromatic anchor of the second transmembrane helix determines the signaling properties of the aspartate/maltose chemoreceptor Tar of *Escherichia coli*, Biochemistry 51 (2012) 1925–1932.
[57] C.A. Adase, R.R. Draheim, G. Rueda, R. Desai, M.D. Manson, Residues at the cytoplasmic end of transmembrane helix 2 determine the signal output of the TarEc chemoreceptor, Biochemistry 52 (2013) 2729–2738.
[58] R.Z. Lai, A.F. Bormans, R.R. Draheim, G.A. Wright, M.D. Manson, The region preceding the C-terminal NWETF pentapeptide modulates baseline activity and aspartate inhibition of *Escherichia coli* Tar, Biochemistry 47 (2008) 13287–13295.
[59] P. Dunnill, The use of helical net-diagrams to represent protein structures, Biophys. J. 8 (1968) 865–875.
[60] C.L. Careaga, J.J. Falke, Structure and dynamics of *Escherichia coli* chemosensory receptors. Engineered sulfhydryl studies, Biophys. J. 62 (1992) 209–216 (discussion 217-209).
[61] V.N. Balaji, A. Mobasser, S.N. Rao, Modification of protein stability by introduction of disulfide bridges and prolines: geometric criteria for mutation sites, Biochem. Biophys. Res. Commun. 160 (1989) 109–114.
[62] N. Srinivasan, R. Sowdhamini, C. Ramakrishnan, P. Balaram, Conformations of disulfide bridges in proteins, Int. J. Pept. Protein Res. 36 (1990) 147–155.
[63] M.P. Leatham-Jensen, J. Frimodt-Moller, J. Adediran, M.E. Mokszycki, M.E. Banner, J.E. Caughron, K.A. Krogfelt, T. Conway, P.S. Cohen, The streptomycin-treated mouse intestine selects *Escherichia coli* envZ missense mutants that interact with dense and diverse intestinal microbiota, Infect. Immun. 80 (2012) 1716–1727.
[64] J. Adediran, M.P. Leatham-Jensen, M.E. Mokszycki, J. Frimodt-Moller, K.A. Krogfelt, K. Kazmierczak, L.J. Kenney, T. Conway, P.S. Cohen, An *Escherichia coli* Nissle 1917 missense mutant colonizes the streptomycin-treated mouse intestine better than the wild type but is not a better probiotic, Infect. Immun. 82 (2014) 670–682.
[65] S.C. Botelho, K. Enquist, G. von Heijne, R.R. Draheim, Differential repositioning of the second transmembrane helices from *E. coli* tar and EnvZ upon moving the flanking aromatic residues, Biochim. Biophys. Acta 1848 (2015) 615–621.
[66] J.J. Falke, G.L. Hazelbauer, Transmembrane signaling in bacterial chemoreceptors, Trends Biochem. Sci. 26 (2001) 257–265.
[67] C. Monzel, G. Unden, Transmembrane signaling in the sensor kinase DcuS of *Escherichia coli*: a long-range piston-type displacement of transmembrane helix 2, Proc. Natl. Acad. Sci. U. S. A. 112 (2015) 11042–11047.
[68] S.D. Goldberg, G.D. Clinthorne, M. Goulian, W.F. DeGrado, Transmembrane polar interactions are required for signaling in the *Escherichia coli* sensor kinase PhoQ, Proc. Natl. Acad. Sci. U. S. A. 107 (2010) 8141–8146.
[69] R. Yusuf, R.R. Draheim, Employing aromatic tuning to modulate output from two-component signaling circuits, J. Biol. Eng. 9 (2015) 7.
[70] J.J. Falke, Piston versus scissors: chemotaxis receptors versus sensor his-kinase receptors in two-component signaling pathways, Structure 22 (2014) 1219–1220.
[71] S. Unnerstale, L. Maler, R.R. Draheim, Structural characterization of AS1-membrane interactions from a subset of HAMP domains, Biochim. Biophys. Acta 1808 (2011) 2403–2412.
[72] A. Rampersaud, M. Inouye, Procaine, a local anesthetic, signals through the EnvZ receptor to change the DNA binding affinity of the transcriptional activator protein OmpR, J. Bacteriol. 173 (1991) 6882–6888.